

DELPHI Collaboration

DELPHI 2001-070 CONF 498

4 July, 2001

---

## Generalised search for hadronic decays of Higgs bosons with the DELPHI detector at LEP-2

**P. Bambade**

LAL, Orsay

**M. Boonekamp, V. Ruhlmann-Kleider**

CEA, Saclay

**G. Borisov**

CERN

**R. Contri**

INFN Genova

**J. Cuevas**

Universidad de Oviedo, Oviedo

**M. Stanitzki**

Inst. für Exper. Kernphysik, Karlsruhe

**I. van Vulpen**

NIKHEF, Amsterdam

### Abstract

Hadronic decays of Higgs bosons, not necessarily into  $b$ -quarks, have been searched for with the DELPHI experiment, using data collected at LEP-2. Such searches are complementary to the usual standard model Higgs searches and lead to more model-independence. Preliminary results are presented both for the  $hZ$  and  $hA$  production mechanisms, using the  $q\bar{q}q\bar{q}$ ,  $q\bar{q}\nu\bar{\nu}$  and  $q\bar{q}l^+l^-$  ( $l = \mu, e$ ) channels.

Contributed Paper for EPS HEP 2001 (Budapest) and LP01 (Rome)

# 1 Introduction

There are extensions of the standard model in which Higgs bosons have suppressed couplings to  $b$ -quarks. This can occur for specific parameters of the Two Higgs Doublet Model (2HDM) [1], or of the Minimal SuperSymmetric Model (MSSM) [2], as well as in some instances of composite models, where the dominant Higgs decay can be into gluon pairs [3]. Standard model Higgs searches [4] would have a reduced sensitivity in such cases, because of their strong reliance on the identification of the  $b$ -quarks from the Higgs boson decay used to maximize the separating power. Hence it is important to also cover more general scenarios experimentally with dedicated searches in which the information from the flavour of the quarks in the Higgs boson decay is not exploited. With such *flavour blind* searches the model-dependence of our final Higgs results can be reduced.

Two production mechanisms were studied, with the Higgs boson produced either in association with a  $Z$  boson ( $e^+e^- \rightarrow Z^* \rightarrow hZ$ ), or with the CP-odd pseudo-scalar boson,  $A$ , predicted in the 2HDM and MSSM ( $e^+e^- \rightarrow Z^* \rightarrow hA$ ). The final states  $q\bar{q}q\bar{q}$ ,  $q\bar{q}\nu\bar{\nu}$ ,  $q\bar{q}\mu^+\mu^-$ , and  $q\bar{q}e^+e^-$  were analysed to study  $hZ$ , while only the  $q\bar{q}q\bar{q}$  one was used for  $hA$ . Some systematic effects were considered, but are not included in the evaluations presented here. All results are preliminary.

## 2 Search for $hZ$ production

### 2.1 Data and simulation samples

The data samples used were collected by DELPHI in 1999 and 2000, and were clustered around six centre of mass energies (see Table 1).

$\sqrt{s}$ (GeV)	$\mathcal{L}(\text{pb}^{-1})$
191.6	25.8
195.5	76.9
199.5	84.3
201.6	41.1
204.9	83.3
206.7	141.4

Table 1: The centre of mass energies and corresponding luminosities used in the analyses.

One sector of the main tracking device TPC (1/12 of the whole detector) was inactive from the beginning of September 2000, which corresponds to one third of the 2000 data sample. The corresponding small change of sensitivity in this period was taken into account in the evaluation. In the  $q\bar{q}\nu\bar{\nu}$  channel, slightly reduced luminosities were used compared to the other channels, because of tighter quality requirement on the running of the detector applied in this channel.

Signal Monte Carlo samples were produced at all six centre of mass energies with the HZHA generator [5], for all relevant decay modes of the  $Z$  boson ( $q\bar{q}, \nu\bar{\nu}, \mu^+\mu^-, e^+e^-$ ), and for the Higgs boson decaying into pairs of gluons or pairs of strange quarks. Samples were generated for Higgs boson masses ranging from 50 to 110 GeV/ $c^2$  in steps of 5 GeV/ $c^2$ .

Complementary samples with the Higgs boson decaying into either  $c\bar{c}$  or  $b\bar{b}$  were also produced, and used to verify the flavour independence of the results.

## 2.2 General strategy

In the various channels, potentially significant differences in performance are expected between flavours, because of differences in jet structure and mass resolution. For each Higgs boson mass hypothesis, the sample used for the final evaluation was conservatively chosen as that which gave the weakest expected exclusion potential, considered globally with all centre of mass energies combined.

Moreover, since the mass resolution in several of the channels is smaller than the 5 GeV/ $c^2$  step between the tested masses, a small degradation of performance was introduced in the final evaluation, between test masses. The magnitude of this degradation, estimated by studying the expected exclusion potential for neighbouring test masses, also considered globally with all centre of mass energies combined, amounted to a maximum 2.5% relative loss of efficiency, for the masses farthest away from the generated test masses.

## 2.3 Four jets

The probabilistic selection used to analyse the four jet channel in the  $e^+e^- \rightarrow ZZ$  production measurement [6, 7, 8] was adapted to test the hypothesis of Higgs boson production independently of the flavour of its decay products. A combined variable was constructed to select the signal at each test mass based on topological information and on the specific invariant mass information, following the method described in [9]. The  $b$ -tagging information was used in the formulation of this variable, but only for jets assigned to the  $Z$  boson. Examples of the resulting probability distributions are shown in Figure 1, for Higgs boson masses of 50, 70, 90 and 105 GeV/ $c^2$ , respectively, adding the events from both years. As can be seen in these distributions, the dominant background depends on the tested mass.  $ZZ$  production dominates the high purity region as expected for the 90 GeV/ $c^2$  mass hypothesis, and QCD processes  $qqgg$  are generally quite important elsewhere. Although these distributions show reasonable overall agreement, there is some excess of events in data in the moderately to high purity region at all test masses up to 100 GeV/ $c^2$ . This excess is thought to originate from an underestimation of the four jet cross-section originating from QCD processes in the simulation [10].

## 2.4 Jets and missing energy

The Iterated Discriminant Analysis (IDA) [11] used in the search for Higgs bosons decaying into invisible modes [12] was adapted to test the hypothesis of Higgs boson production in the missing energy channel independently of the flavour of its decay products. The optimization was done separately for masses above and below 80 GeV/ $c^2$  so as to ensure good performance in both ranges. After a preselection consisting of cuts applied to remove  $\gamma\gamma$  and  $Z\gamma$  processes [12], twelve discriminating variables were combined into a single one using the IDA method [11]. As in the search for Higgs bosons decaying into invisible modes, this procedure was repeated a second time after an enrichment cut on the combined variable obtained in the first step, in order to concentrate the optimisation

on the signal region. The combined variable obtained in this second step and the reconstructed mass were then used to select the signal. The mass information was taken into account through a set of cuts applied to isolate the contribution from the  $hZ$  signal, for each of the thirteen test masses, optimized considering both the varying mass resolution of the signal and the shape and changing level of the residual background. For each of the mass hypotheses, after the corresponding mass cuts, the distribution of the combined variable from the second step was used. Examples of such distributions are shown in Figure 2, for Higgs boson masses of 50, 70, 90 and 105 GeV/ $c^2$ . Although these distributions show reasonable general agreement, a moderate overall deficit of events in the data can be observed with respect to the simulation. This deficit, which may be of statistical or systematic nature, is however global and is not concentrated in the high purity bins of the distributions which correspond to the signal-like region.

## 2.5 Jets and a pair of isolated leptons

The  $q\bar{q}e^+e^-$  and  $q\bar{q}\mu^+\mu^-$  channels were analysed in the same way as in the  $e^+e^- \rightarrow ZZ, Z\gamma^*$  production measurements [6, 7, 8, 13]. Events were selected by sequential cuts, initially without explicit condition on the invariant mass of the lepton and quark system. The particle identification criteria were carefully tuned to maximise the efficiency of selecting leptons and the signal to background ratio. Sets of mass cuts were then applied to isolate the contribution from the  $hZ$  signal, for each of the thirteen test masses, taking into account both the varying mass resolution of the signal and the changing background level from the  $ZZ$  and  $Z\gamma^*$  processes which dominate these topologies. The numbers of events selected in data and in the simulation in both years are shown in Figure 3 and Figure 4 as a function of the tested mass, for the  $q\bar{q}e^+e^-$  and  $q\bar{q}\mu^+\mu^-$  channels, respectively. The observed distributions are in reasonable agreement with the predictions from simulation. Signal efficiencies, evaluated for each test mass and centre of mass energy, were around 75 and 65 % for each of the two channels, respectively.

## 2.6 Results

No evidence for  $hZ$  production was found at any of the masses tested, in any of the channels studied. Constraints on the production of Higgs bosons independently of the flavour of the Higgs boson decays were computed by combining the information from all channels, using two independent methods.

In a first stage, upper limits on the production cross-sections were determined by means of maximum likelihood fits to the signal hypothesis corresponding to each test mass, following a procedure used in the  $ZZ$  production measurement [6, 7, 8]. In these fits, all the bins of the combined variables constructed for the  $q\bar{q}q\bar{q}$  and  $q\bar{q}\nu\bar{\nu}$  channels, and the numbers of events selected in the  $q\bar{q}\mu^+\mu^-$  and  $q\bar{q}e^+e^-$  channels, were used, adding together the information from the different centre of mass energies. It was shown that the signal purities in these different bins were close enough to being independent of the centre of mass energy, so as to cause only moderate dilution of the information. The global likelihood functions obtained were then integrated over a large range of positive signal cross-sections to compute both expected and observed excluded cross-section values at 95% confidence level. The results of this procedure are shown in Figure 5 as a function of the tested mass. Cross-sections larger than about half the expected standard model value

are excluded up to  $100 \text{ GeV}/c^2$ . In the assumption of a production cross-section equal to that of the standard model, the observed and expected lower limits on the mass obtained by this procedure are  $109$  and  $108 \text{ GeV}/c^2$ , respectively.

The 95% confidence level observed and expected lower limits on the mass were also computed with the likelihood ratio technique [14] used in the evaluation of the standard model Higgs boson search [4]. The confidence levels from this calculation are shown as a function of the mass in Figure 6a,b for the signal and background-only hypotheses, respectively. The observed and expected limits obtained were  $109.9$  and  $109.1 \text{ GeV}/c^2$ , respectively. These numbers are the final result of this search. The six centre of mass energies were treated separately in this computation: this partly explains the slightly stronger results obtained in comparison with the method based on the maximum likelihood fit.

### 3 Search for $hA$ production

#### 3.1 Data and simulation samples

The data samples used in this analysis were collected by DELPHI at  $189 \text{ GeV}$  in 1998,  $196$  and  $200 \text{ GeV}$  in 1999, and above  $204.5 \text{ GeV}$  in the year 2000. The total corresponding luminosity amounted to  $523 \text{ pb}^{-1}$ .

Signal samples were produced with the HZHA generator [5] at centre-of-mass energies of  $189$ ,  $196$ ,  $200$  and  $206 \text{ GeV}$ , in the range  $m_h, m_A > 15 \text{ GeV}/c^2$  and  $180 > m_h + m_A > 40 \text{ GeV}/c^2$ , using a grid of step  $5 \text{ GeV}/c^2$  if one of the masses was below  $30 \text{ GeV}/c^2$ , and  $10 \text{ GeV}/c^2$  if both were above. For reasons explained below, the main decay mode was chosen as  $hA \rightarrow 4$  gluons. For some fraction of the  $h$  and  $A$  test masses, decays into four light quarks were produced in addition.

#### 3.2 General strategy

The search for  $hA$  production in the flavour blind hypothesis was designed to cover a large part of the kinematically accessible  $h$  and  $A$  mass range, and was based on general kinematic features such as event shapes and detailed mass information. In order to ensure flavour independent results, two sizeable and competing effects arising from the different hadronization of quarks and gluons had to be considered: the higher multiplicity of gluon jets on one side, and the better dijet mass resolution of quark jets on the other side. In order to minimize biases which may arise from these effects, the multiplicity selection and corresponding efficiency were determined using  $hA \rightarrow$ light quarks samples, while the mass reconstruction was evaluated with  $hA \rightarrow$ gluons samples.

#### 3.3 Analysis streams

A first preselection was applied to all events, requiring them to have at least 20 charged tracks, a total reconstructed energy in excess of  $100 \text{ GeV}$ , and an effective centre-of-mass energy after initial state radiation greater than  $150 \text{ GeV}$ . The efficiencies of the multiplicity cut were typically 98% and 100% for the  $hA \rightarrow$ light quarks and  $hA \rightarrow$ gluons samples, respectively. In the rest of the analysis, it was necessary to consider separately

three different topologies, in order to achieve good performance over a large range in the  $m_h - m_A$  plane, as described below.

### Four jets

Close to the kinematic limit and when both Higgs bosons have similar masses, a four jet topology is expected. To analyse this topology, events were clustered into four jets and retained if their thrust was below 0.85 and if the product of the smallest jet energy and interjet angle (called  $E_{\min}\alpha_{\min}$ ) was greater than 10 GeV $\times$ rad. Dijet invariant mass information was used to reject events compatible with  $WW$  production as in [9], requiring the corresponding probability, called  $P_{WW}$ , to be less than 0.03. This proved helpful not only in the case of  $m_h = m_A \sim 80$  GeV/ $c^2$  but also for other masses, where  $WW$  production contributes to the expected background through wrong jet pairings.

### Three jets

With increasing mass difference, the events tend to become more three jet-like, since the decay jets of the lighter Higgs boson are not always resolved. The same behaviour is observed if  $h$  and  $A$  both have low masses, because of the larger boost in this case. To analyse this topology, only events with thrust values between 0.7 and 0.9 were kept. Events were firstly clustered into four jets, and the compatibility with  $WW$  production was then tested as in the four jet stream. The remaining events were clustered into three jets.

### Three jets with high thrust

Finally, if both Higgs bosons are very light (below 30 to 40 GeV/ $c^2$ ), signal events tend to become cigar-like. In this case, the events were required to have a thrust  $\geq 0.93$ , and were clustered into three jets as above.

Distributions of the variables used are shown in Figure 7 for the typical masses relevant to these three analysis streams. Their performances and complementarity are illustrated in Table 2, where typical mass-averaged efficiencies, obtained for the different categories of signal events, are summarised. The numbers of observed data and expected background events are shown in Table 3. The remaining flavour dependence at this stage was less than 3%.

	$\epsilon(4 - \text{jet})$	$\epsilon(3 - \text{jet})$	$\epsilon(\text{high} - \text{thrust})$
four-jet events	$\sim 70\%$	$\sim 45\%$	0 – 5%
three-jet events	$\sim 50\%$	$\sim 70\%$	0 – 5%
high-thrust events	0 – 5%	0 – 5%	10 – 15%

Table 2: Efficiencies of the three analysis streams applied to three classes of signal events defined as follows: *Four-jet*: both  $m_h$  and  $m_A > 60$  GeV/ $c^2$ ; *high-thrust*: both  $m_h$  and  $m_A < 30$  GeV/ $c^2$ ; *three-jet*: remaining cases.

Centre of mass energy	189 GeV	196 GeV	200 GeV	>204.5 GeV
Four-jet stream :				
Expected background	436.6	230.5	248.0	652.6
Observed events	459	248	232	642
Three-jet stream :				
Expected background	800.2	405.7	406.9	923.8
Observed events	798	413	398	942
High-thrust stream :				
Expected background	955.6	461.6	422.5	1137.3
Observed events	954	420	412	1072

Table 3: Numbers of observed and expected background events for the four data sets considered and for the three analysis streams.

### 3.3.1 Final discriminant

In all three analysis streams, a four-constraint fit was performed on the events, requiring total energy and momentum conservation. A discriminant variable was then built from the reconstructed jet and dijet masses and their errors, by minimising the following quantity:

$$\chi^2(m_{1,test}, m_{2,test}) = \left[ \left( \frac{|m_{1,rec} - m_{1,test}|}{\delta m_{1,rec}} \right)^2 + \left( \frac{|m_{2,rec} - m_{2,test}|}{\delta m_{2,rec}} \right)^2 \right],$$

defined for each event, over the available pairing combinations. In the above expression,  $m_{1,rec}$  is the mass of a given dijet,  $m_{2,rec}$  is the mass of the opposite dijet in the four-jet stream, and of the opposite jet in the other streams, and  $\delta m_{1,2}$  are the corresponding errors. This discriminant variable was computed for the data, background and signal, for each test mass configuration  $(m_{1,test}, m_{2,test})$ , on a  $2 \times 2$  GeV/ $c^2$  grid in the  $(m_h, m_A)$  plane and projected into histograms as illustrated in Figure 8. These histograms were used for the statistical evaluation of the compatibility of the data with the simulation, by combining the Poisson probabilities from each bin, following the procedure described in [15]. The overlap between the selections in the three- and four-jet streams was removed at this stage by choosing the strongest one for each mass point, based on the expected performance.

## 3.4 Results

Figure 9 shows the excluded region in the  $(m_h, m_A)$  plane, when the coupling of  $hA$  to the  $Z$  boson is maximal. The complementarity of the three analysis streams is clearly visible. The first analysis of this kind, performed by the OPAL collaboration [16], considered only four-jet topologies, and was therefore sensitive only to  $h$  and  $A$  masses above 30 GeV/ $c^2$ : the present analysis allows further exploration. The unexcluded region lying roughly along the  $m_h + m_A = 70$  GeV/ $c^2$  line is due to the transition between the high-thrust and three-jet streams. Improvement in this region is expected in the near future.

Finally, the flavour-blind  $hA$  search was also used to extend the reach of the previously described  $hZ$  search, to Higgs boson masses below 50 GeV/ $c^2$ . If one fixes the  $A$  mass equal to the  $Z$  mass, one can test the compatibility of the data with the prediction for

various  $m_h$  hypotheses, using the three-jet stream most adapted to this mass range. Figure 10 shows the  $hZ$  cross-section (in units of the standard model value) excluded in this way. It is obtained by testing the data every 2 GeV/ $c^2$  in  $m_h$ , between 15 and 90 GeV/ $c^2$ . Above roughly 50 GeV/ $c^2$ , the analysis sensitivity breaks down as the three-jet stream is no longer appropriate. Cross-section larger than 10-20 % of the standard model value are typically excluded in the mass range between 15 and 50 GeV/ $c^2$ .

## 4 Summary and conclusions

DELPHI has searched for Higgs bosons at LEP-2 without exploiting the flavour of its decays. No signal was found in either of the two main production mechanisms  $e^+e^- \rightarrow Z^* \rightarrow hZ$  and  $hA$  studied, in a broad range of masses extending from 15 GeV/ $c^2$  to close to the kinematic limit.

For the  $hZ$  process, cross-sections larger than about 10-60 % of the expected standard model values were excluded in the range of masses from 15 to 100 GeV/ $c^2$ , independent of the flavour of the Higgs boson decays. In the assumption of a production cross-section equal to that of the standard model, lower observed and expected mass limits of 109.9 GeV/ $c^2$  and 109.1 GeV/ $c^2$  were set, respectively.

For the  $hA$  process, a large part of the available mass range was excluded, extending roughly from  $m_{h,A} = 15$  to  $m_{h,A} = 120$  GeV/ $c^2$  (for  $m_h + m_A < 140$  GeV/ $c^2$ ), independent of the flavour of the Higgs boson decays, in the assumption of production cross-sections equal to the maximum value allowed by electroweak symmetry breaking.

These results are all preliminary, and will be improved in the future thanks to better optimizations, more precise studies of systematic effects, and a more uniform and comprehensive evaluation of the statistical confidence intervals. Flavour independent Higgs boson searches performed by other LEP collaborations can be found in [17]. Results obtained for the  $hZ$  process by the four LEP collaborations have also been combined recently - see [18].

## Acknowledgements

We are greatly indebted to our technical collaborators, to the members of the CERN-SL Division for the excellent performance of the LEP collider, and to the funding agencies for their support in building and operating the DELPHI detector.

## References

- [1] J. F. Gunion, H. E. Haber, G. L. Kane and S. Dawson *The Higgs Hunter's Guide*, Addison-Wesley Publishing Company, 1990
- [2] M. Carena, S. Heinemeyer, C. E. Wagner and G. Weiglein, Suggestions for improved benchmark scenarios for Higgs-boson searches at LEP2, hep-ph/9912223.  
M. Carena, S. Mrenna and C. E. Wagner, *Phys. Rev. D* **60** (1999) 075010  
W. Loinaz and J. D. Wells, *Phys. Lett. B* **445** (1998) 178  
M. Carena, J. Ellis, A. Pilaftsis, C. E. Wagner *Nucl. Phys.* **B586** (2000) 92



- [3] X. Calmet and H. Fritzsch, Phys. Lett. B **496** (2000) 190
- [4] DELPHI Collaboration, Phys. Lett. B **499** (2001)23)
- [5] P. Janot, in CERN Report 96-01, Vol. 2, p. 309.
- [6] DELPHI Collaboration, Phys. Lett. B **497** (2001) 199.
- [7] DELPHI Collaboration, *Update of ZZ production measurement in  $e^+e^-$  interactions using data at 192-202 GeV*, Contribution to the HEP conference in Osaka, Japan, 2000, DELPHI 2000-145 CONF 444.
- [8] DELPHI Collaboration, *Update of the ZZ cross-section measurement in  $e^+e^-$  interactions using data collected in 2000*, Contribution to the EPS conference in Budapest, Hungary, 2001, DELPHI 2001-105 CONF 533.
- [9] I. Van Vulpen and N. Kjaer, DELPHI 99-169 PHYS 839 (1999).
- [10] A. Ballestrero *et al.*, hep-ph/0006259.
- [11] T.G.M. Malmgren, Comp. Phys. Comm. **106** (1997) 230;  
T.G.M. Malmgren and K.E. Johansson, Nucl. Inst. Meth. **403** (1998) 481.
- [12] DELPHI Collaboration, *Searches for invisibly decaying Higgs bosons*, Contribution to the summer conferences, DELPHI 2001-079 CONF 507.
- [13] DELPHI Collaboration, *Measurement of the production of the four-fermion final states mediated by neutral current processes*, Contribution to the EPS conference in Budapest, Hungary, 2001, DELPHI 2001-096 CONF 524.
- [14] A. L. Read, in CERN Report 2000-005, p. 81 (2000).
- [15] V.F. Obraztsov, Nucl. Instr. Meth. **A316** (1992) 388, and Erratum in Nucl. Instr. Meth. **A399** (1997) 500.
- [16] OPAL Collaboration Eur. Phys. J. **C18** (2001) 425-445
- [17] ALEPH Collaboration, *A flavour independent search for the Higgsstrahlung process in  $e^+e^-$  collisions at centre-of-mass energies from 189 to 209 GeV*, CONF-2001-018 ALEPH 2001-021,  
L3 Collaboration, *Search for Production of Neutral Higgs Scalars in  $e^+e^-$  Annihilations at LEP*, L3 note 2576 (2000),  
OPAL Collaboration, *Searches for Higgs Bosons in Extensions to the Standard Model in  $e^+e^-$  Collisions at the Highest LEP Energies*, OPAL Physics Note PN-472 (2001),  
OPAL Collaboration, *Model Independent Searches for Scalar Bosons with the OPAL Detector at LEP*, OPAL Physics Note PN-449 (2000),  
OPAL Collaboration, Eur. Phys. J. **C18** (2001) 425-445.
- [18] The LEP Working Group for Higgs Boson searches, *Generalised search for hadronic decays of Higgs bosons at LEP-2*, Contribution to the EPS conference in Budapest, Hungary, 2001, LHWG note 2001-07

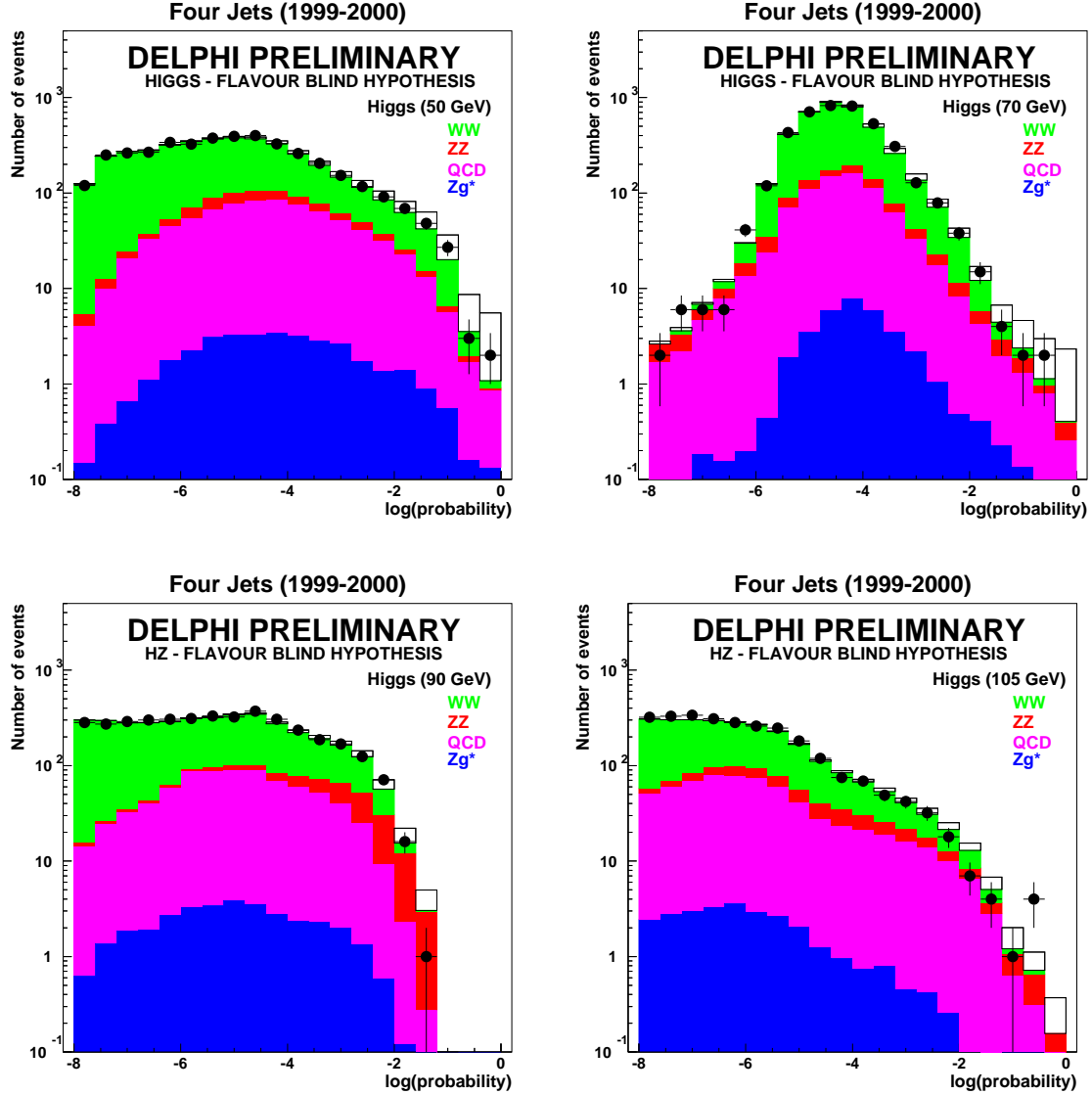


Figure 1: Distributions of the combined probabilities constructed in the hypotheses of  $hZ$  production for Higgs boson masses of 50, 70, 90 and 105 GeV, by combining invariant mass, topological and jet  $b$ -tagging information (only for the jets assigned to the  $Z$  boson), as well as the predicted standard model cross-sections and branching ratios into the different quark configurations (see [6, 9]). The data from the six centre of mass energies in 1999 and 2000 are shown together. It has been shown that these variables give good estimates of the actual probabilities to select events in the corresponding hypotheses, and that the different energies can therefore be added in the evaluation with only limited dilution.

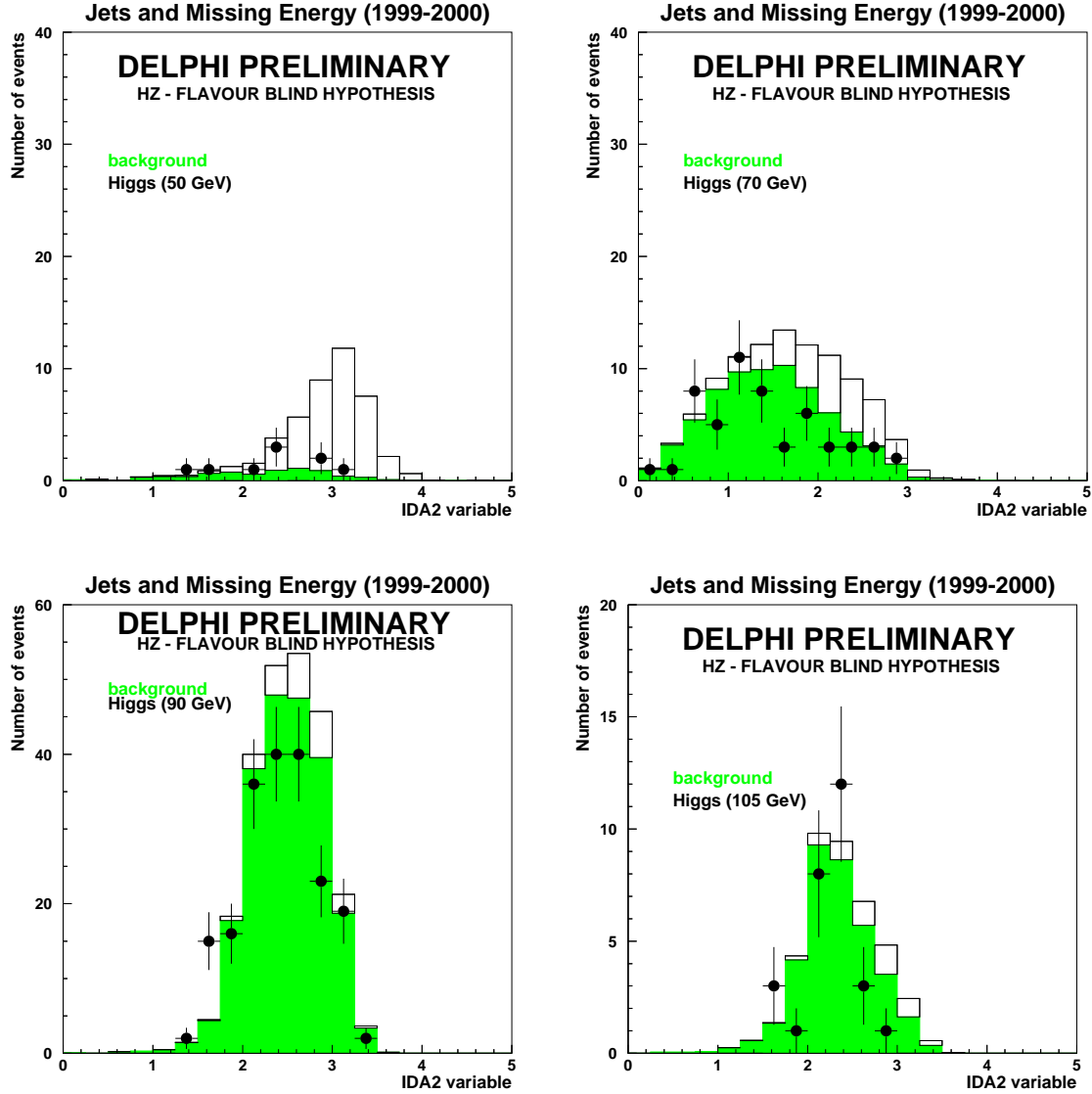


Figure 2: Distributions of the discriminant variables constructed to select  $hZ$  events in the missing energy channel independently of the flavour of the Higgs decays, obtained after a set of mass cuts optimized to maximize the separating power for each tested mass. The distributions shown correspond to Higgs boson masses of 50, 70, 90 and 105 GeV, with the data from all six centre of mass energies in 1999 and 2000 added. It has been shown that the signal purities in the bins of these variables are close to independent of the centre of mass energy, and that the evaluation can therefore be performed with moderate dilution using these combined distributions.

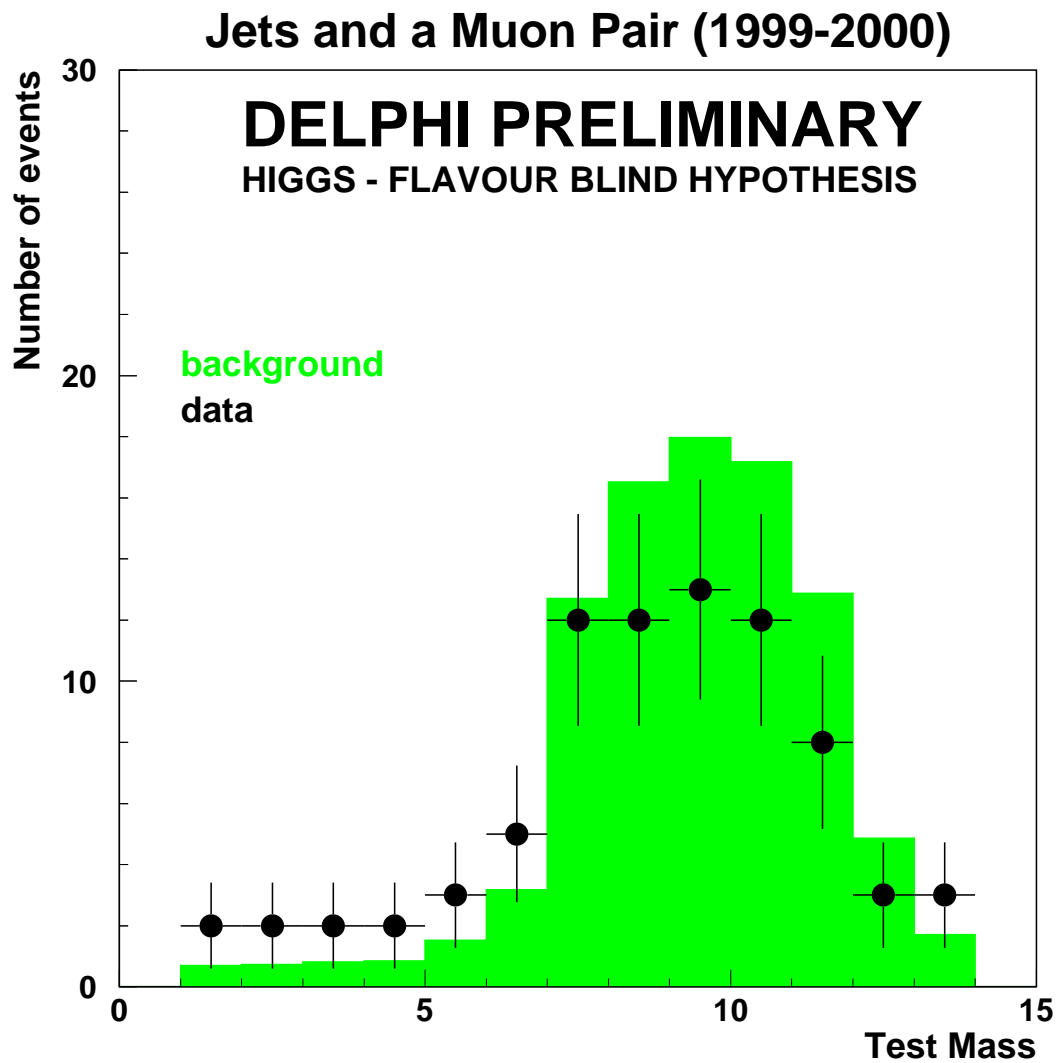


Figure 3: Number of  $q\bar{q}\mu^+\mu^-$  events selected in data and in the simulation in 1999 and in 2000 as a function of the tested mass. The main background contributions are from  $ZZ$  and  $Z\gamma^*$  processes.

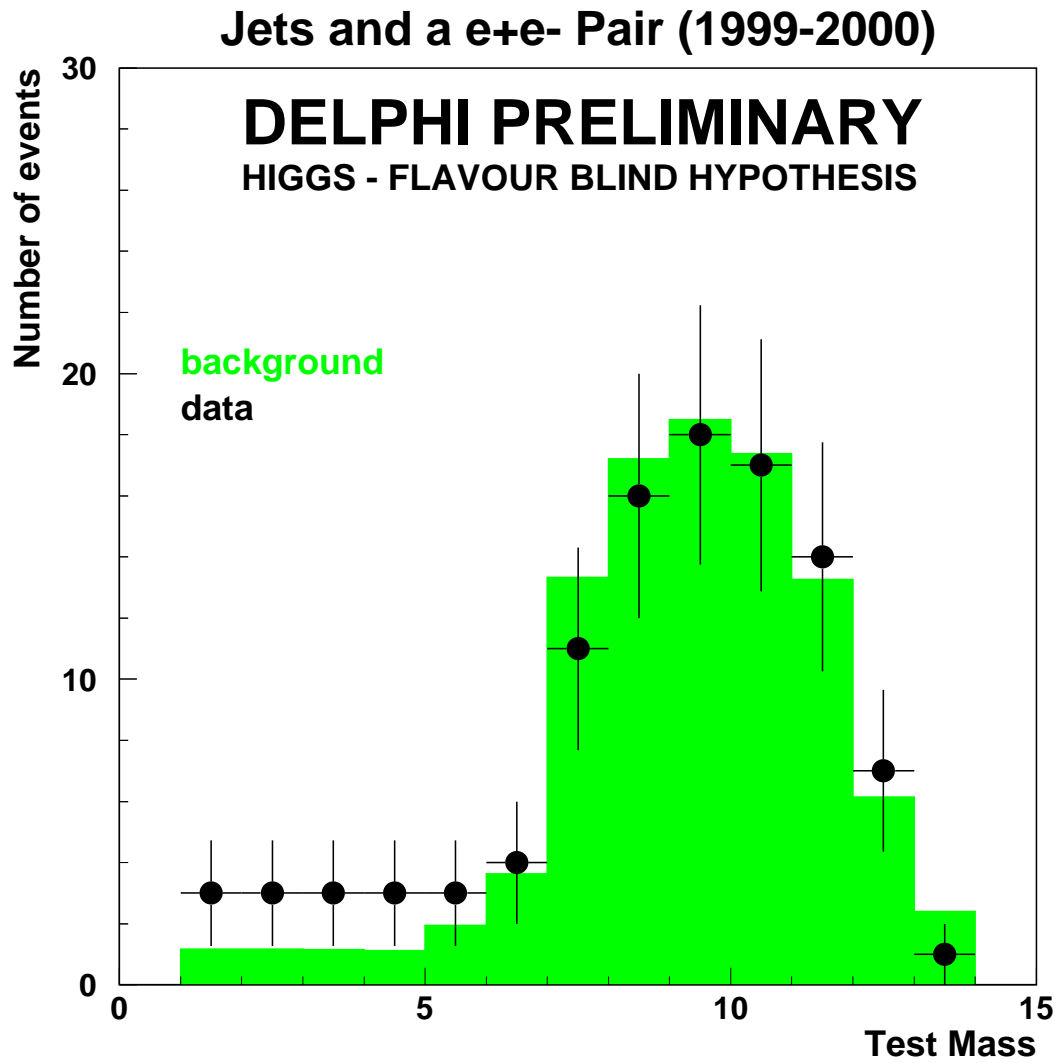


Figure 4: Number of  $q\bar{q}e^+e^-$  events selected in data and in the simulation in 1999 and in 2000 as a function of the tested mass. The main background contributions are from  $ZZ$ ,  $Z\gamma^*$  and  $Zee$  processes.

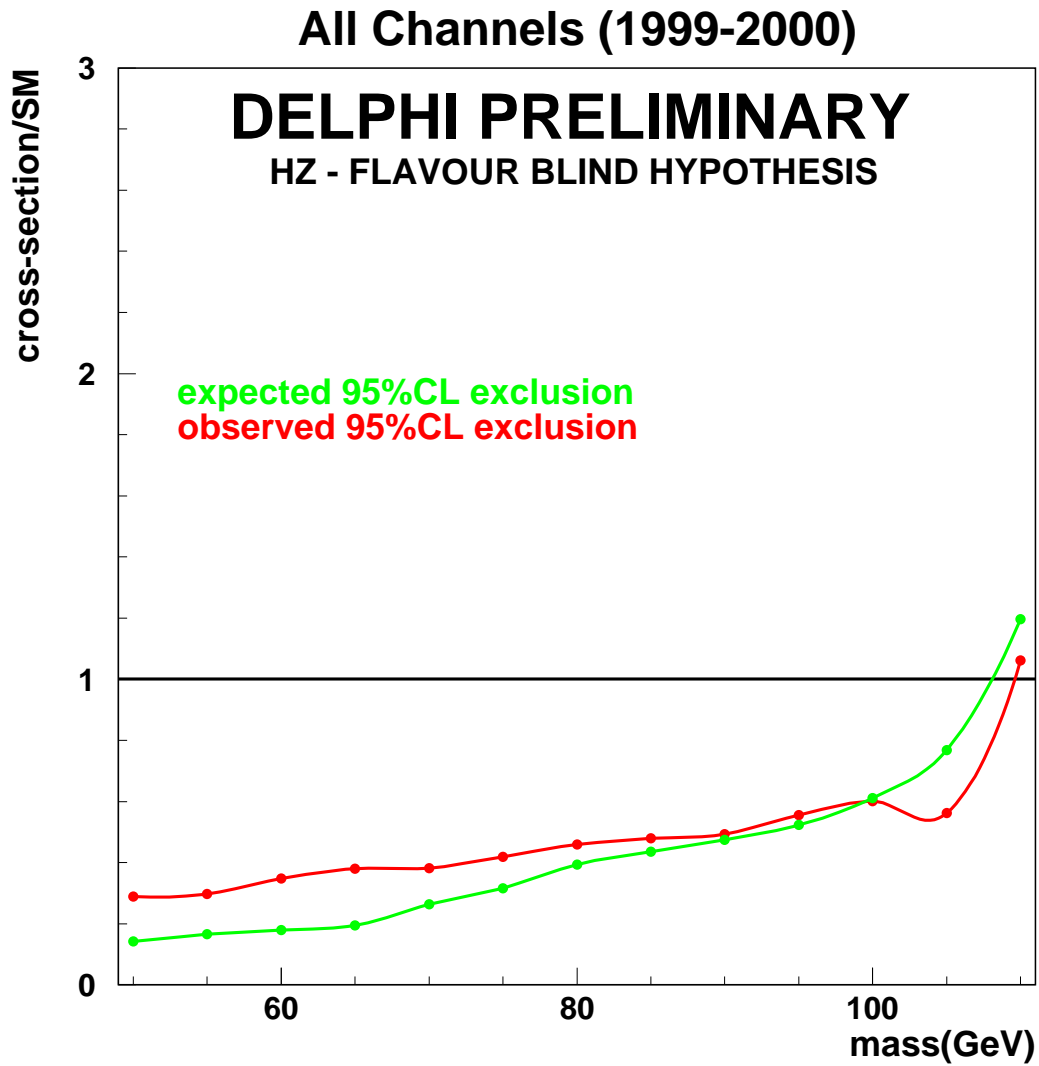
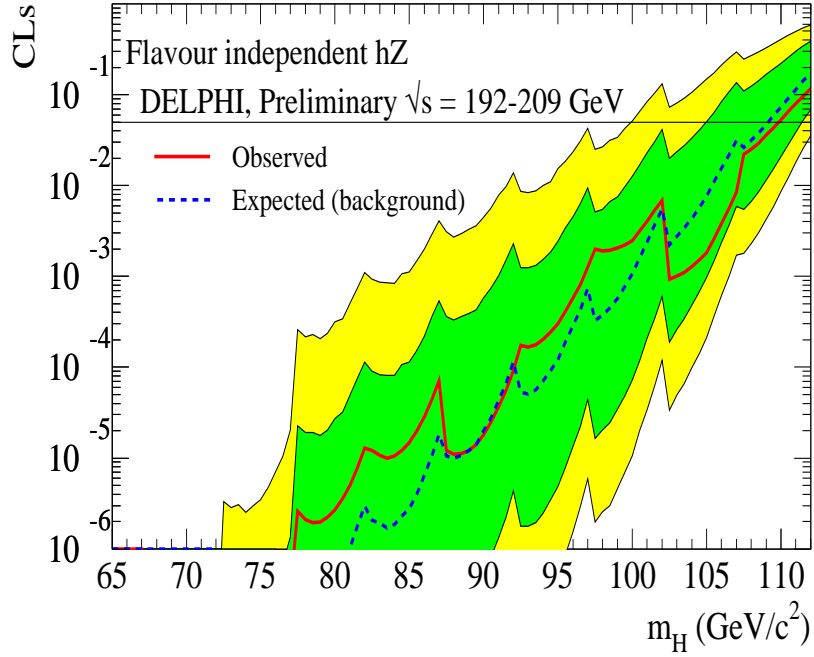


Figure 5: Observed and expected upper limits on the production cross-sections determined by means of maximum likelihood fits to the signal hypotheses corresponding to each test mass, following the procedure used in the  $ZZ$  production measurement [6, 7, 8]. The fits were performed only for the thirteen test masses (see the text), and lines were drawn between the points.

a)



b)

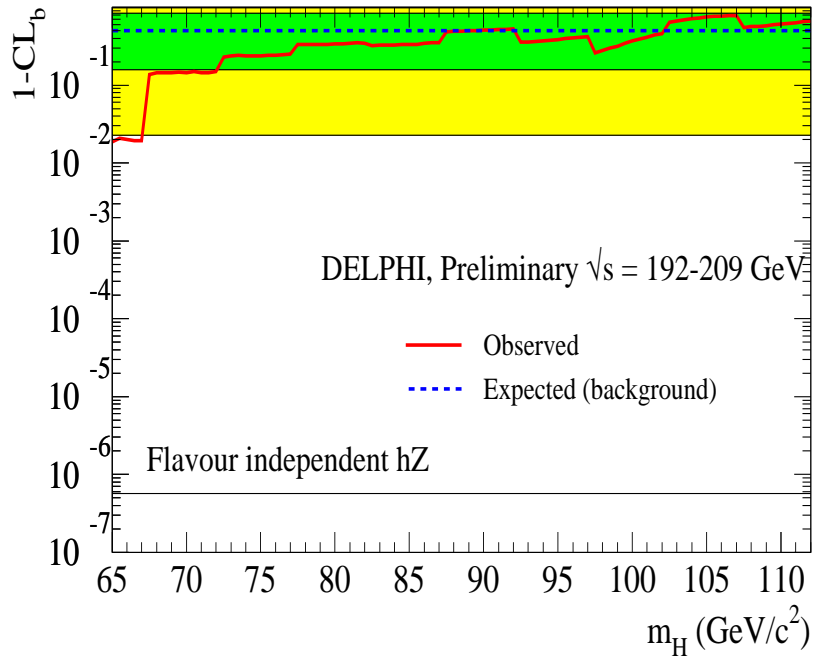


Figure 6: Confidence levels as a function of the Higgs boson mass, computed with the likelihood ratio technique [14] used in the evaluation of the standard model Higgs boson search [4]. Curves are the observed (solid) and expected median (dashed) confidences from background-only experiments, while the bands correspond to 68.3 % and 95 % confidence intervals from the background-only experiments. The confidence levels for the signal and background-only hypotheses are shown in the upper (a) and lower (b) plots, respectively. The spikes visible in the confidence level for the signal hypothesis are an artefact of the 2.5% relative loss of efficiency introduced to take into account the expected degradation of performance in between the generated test masses (see the text).

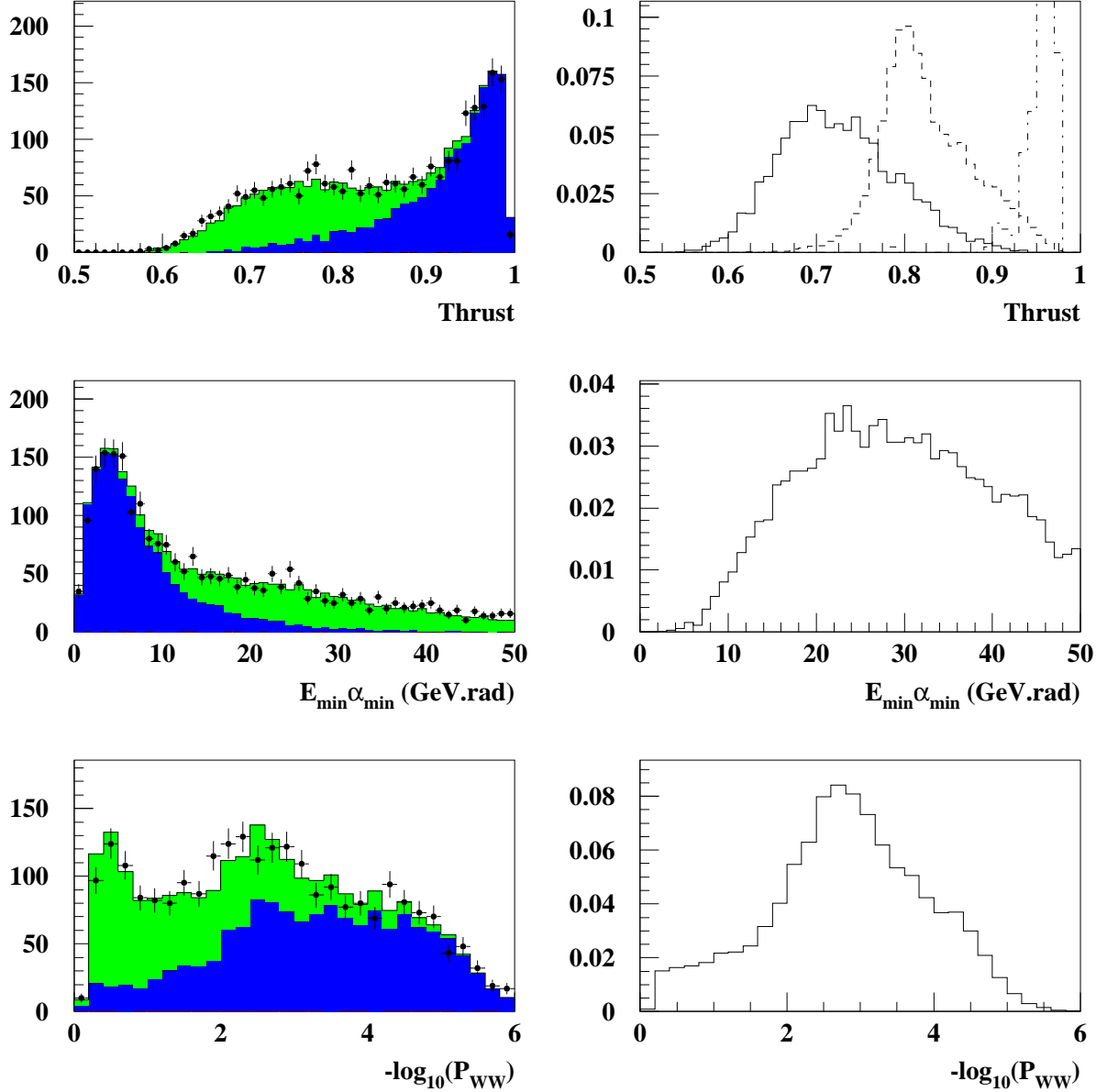


Figure 7: hA search: data to Monte-Carlo comparisons for the variables used in the three selection streams. On the right part, the dots represent the data, the light (resp. dark) histogram corresponds to the expected 4-fermion (resp. 2-fermion) background. The discriminating power is shown for three representative signals in the case of thrust ( $m_h, m_A = 70,70$  ;  $70,30$  ;  $30,30$  GeV from lower to higher thrust), and for  $m_h, m_A = 70,70$  GeV in the case of  $E_{\min}\alpha_{\min}$  and  $-\log_{10}(P_{\text{WW}})$ .



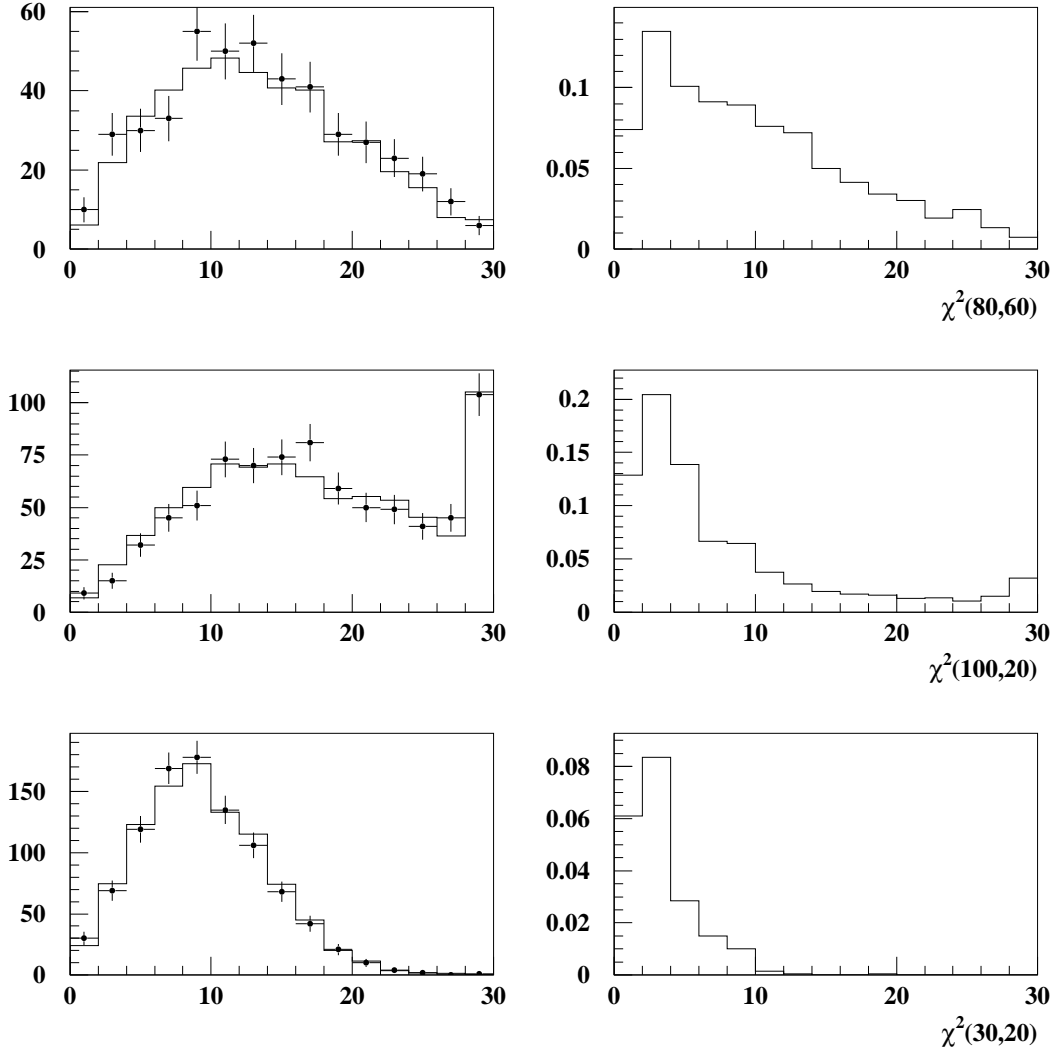


Figure 8: hA search: distributions of the variable  $\chi^2(m_1, m_2)$  for the data and expected background (left) and signals (right). The upper figure shows the discrimination obtained for a  $m_h, m_A = 80, 70$  hypothesis in the four-jet stream. The middle figure shows the discrimination obtained for a  $m_h, m_A = 100, 20$  hypothesis, in the three-jet stream. The lower figure show the discrimination obtained for a  $m_h, m_A = 30, 20$  hypothesis, in the high-thrust stream.

# DELPHI PRELIMINARY

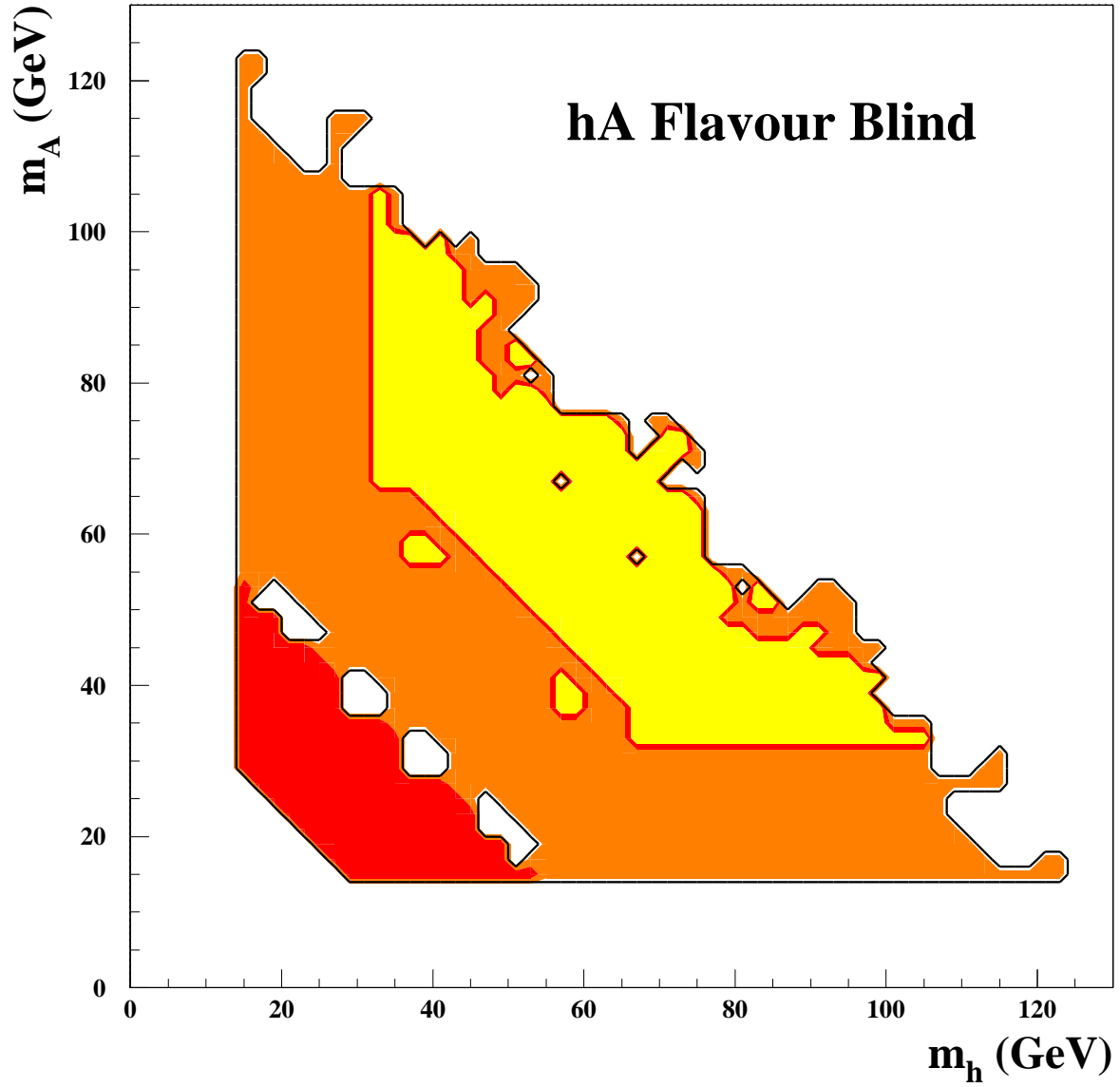


Figure 9: Region excluded in the  $m_h, m_A$  plane, by the high-thrust search, the three-jet search, and the four-jet search, from darker gray to lighter gray respectively. The  $ZhA$  coupling is taken maximal, and 100% branching ratio of  $h$  and  $A$  into hadrons is assumed.

# DELPHI PRELIMINARY

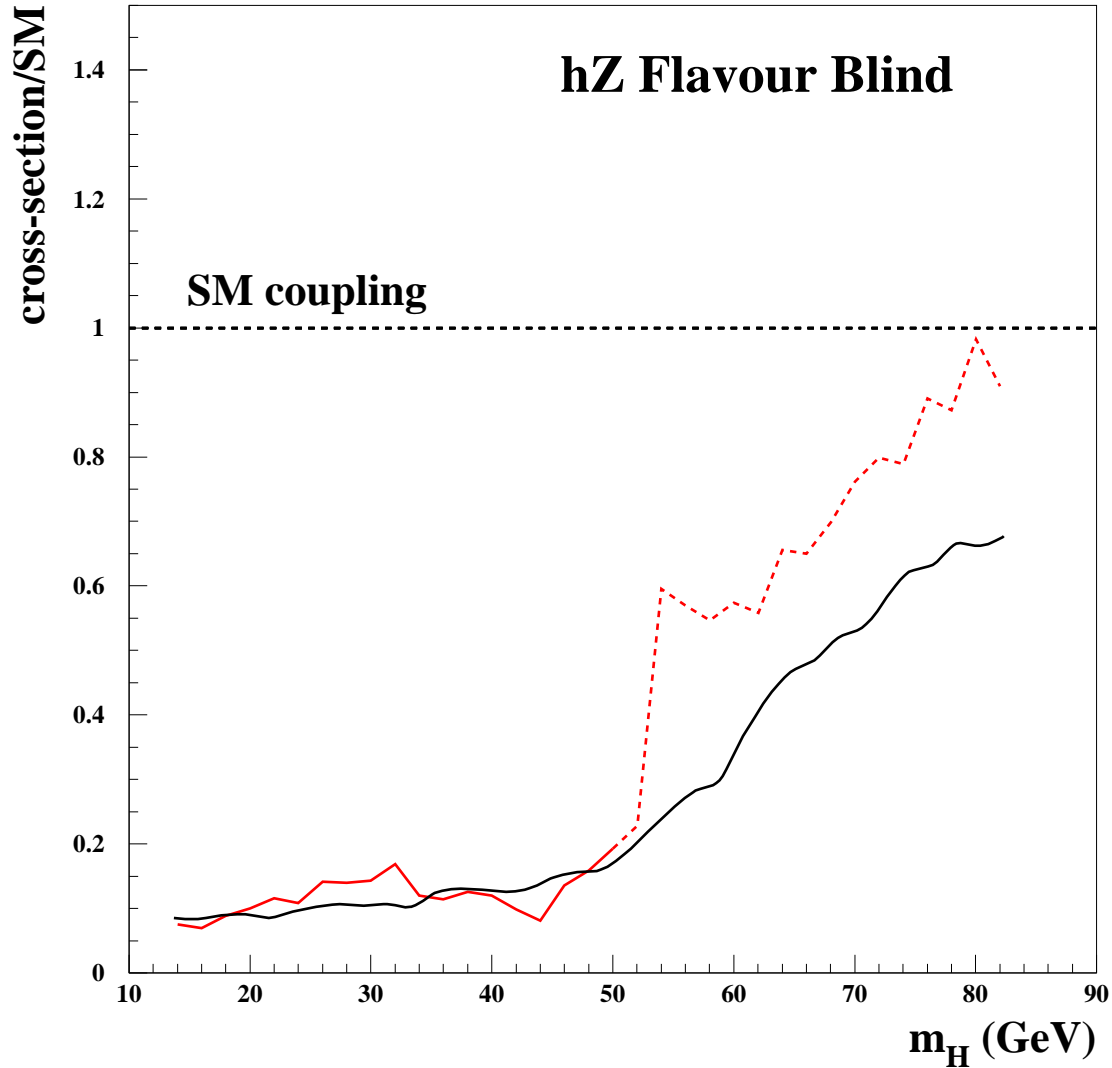


Figure 10: Excluded hZ cross-section in units of the SM cross-section, as a function of  $m_H$ , obtained as an application of the hA three-jet analysis stream with  $m_A$  fixed at  $m_Z$ . The light curve corresponds to the observed excluded cross-section ; the full part corresponds to the region where this analysis is complementary to the dedicated hZ search ; the dashed part shows the breakdown of the analysis at higher Higgs boson masses. The dark curve shows the expected exclusion.